

SEMESTER THESIS

Design and characterization of microwave Printed Circuit Boards for circuit QED experiments

Presented by: Simon Schmidlin
Supervisor: Dr. Peter Leek
Handed-in to: Prof. Dr. Andreas Wallraff,
Laboratory for Solid State Physics, ETH Zürich

Zürich, September 29, 2008

A circuit QED system uses a one-dimensional transmission line resonator and a Cooper pair box as a qubit which can be controlled by the resonator. One has to be able to control the parameters of each qubit individually. This means that one should be able to change the state of a qubit without disturbing the other ones and also to tune the transition frequency of each qubit separately. The qubit transition frequency can be adjusted by a magnetic flux through the loop of the Cooper pair box. Therefore we need a lot of place to accommodate all this in on a device. In this thesis, a set of new PCB's (Printed Circuit Boards) was designed and characterised in order to offer enough place for more complicated circuit designs on it.

Contents

1	Introduction	1
2	Theory	3
2.1	The lumped-element circuit model for a transmission line	3
2.2	Conventional coplanar waveguide	4
2.2.1	Conductor-backed coplanar waveguide	4
2.3	parallel RLC resonant circuit	6
2.4	Loaded and unloaded Q	8
2.5	Open-Circuited $\lambda/2$ Line	8
2.6	Capacitive coupling	9
3	Designs	11
3.1	Materials	12
3.2	Bends	12
3.3	Different sizes and connectivity of the PCB's	12
4	Measurements and characterization	18
4.1	Calibration	18
4.2	Resonator measurements	20
5	Later experiments	25
6	Conclusion	27
7	Appendix	28
7.1	The lumped-element circuit model for a transmission line	28
7.2	The Lossless Line	29
7.3	parallel RLC resonant circuit	29
7.4	Open-Circuited $\lambda/2$ Line	30
7.5	Capacitive coupling	30

1 Introduction

Computer hardware has grown in power at an amazing pace ever since, Gordon Moore states in 1965 that the computer power will double for constant cost roughly once every two years. Amazingly enough, Moore's law has approximately held true in the decades since the 1960s. Nevertheless, most observers expect that this dream run will end some time during the first two decades of the twenty-first century. Conventional approaches to the fabrication of computer technology are beginning to run up against fundamental difficulties of size. Quantum effects are beginning to interfere in the functioning of electronic devices as they are made smaller and smaller. In 1982, Richard Feynman brought up the idea of a quantum computer as a device which takes advantage of the effects of quantum mechanics such that it might perform more powerful calculations than a classical computer. A search for an experimental realization of such a quantum computer and its basic units of information, the quantum bits (qubits) has begun. Qubits do not only take the value 0 or 1 like classical bits, a pure qubit state is a linear superposition of those two states. This means that the qubit can be represented as a linear combination (also called "superposition") of $|0\rangle$ and $|1\rangle$. A qubit can therefore be drawn by a vector contained in a sphere (Bloch sphere). The angle though which the vector is rotated about the vertical axis is a measure of the phase of the qubit. The implementation of such a qubit requires a quantum mechanical two-level system that can be well controlled and measured. There are many possible implementations of such qubits:

- Single photon \rightarrow Polarization of light
- Electrons \rightarrow Spin up/down or electron number
- Optical lattices \rightarrow Atomic spin up/down
- Quantum dot \rightarrow Dot spin up/down
- Josephson junction \rightarrow Un/charged superconducting island ($Q=0/2e$)

A physical state will always have some interaction with its environment. Due to this external influence, a superposition state $(|0\rangle + |1\rangle)/\sqrt{2}$ will have a time-development into the state $|0\rangle$ or $|1\rangle$, which is equivalent to a collapse of the superposition state. This loss of the superposition property of a quantum state is called decoherence. The measurable time of decoherence is denoted by T_2 . This is one of the main problem in building a quantum computers. A good isolation of the qubit from its environment is therefore necessary (beside the preparing and measuring the qubit), such that it has a long decoherence time, which allows to perform many operations before the superposition state is destroyed. An other important time scale is the so called relaxation time: If one leaves a system to its own, it tend to the state of lowest energy. The relaxations time is denoted by T_1 . As a rule, T_1 and T_2 are exponentially distributed. Notice that typically T_2 is much smaller than T_1 .

David DiVincenzo, of IBM, listed the following requirements for a practical quantum computer:

- scalable physically to increase the number of qubits
- qubits can be initialized to arbitrary values
- quantum gates faster than decoherence time
- universal gate set
- each qubit can be read easily

A quantum gate is a basic quantum circuit operating on a small number of qubits. One promising approach toward quantum computers which allows to isolate the qubits efficiently from the environment while still providing good measurement and control possibilities is called circuit quantum electrodynamics (cQED). A charge qubit is formed by a tiny superconducting island (Cooper-pair box) coupled by a Josephson junction to a superconducting reservoir. The state of the qubit is determined by the number of Cooper pairs which have tunneled across the junction. The Cooper pair box is coupled to a microwave cavity, which is realized with a one-dimensional line resonator. By applying microwave signals to the resonator, one can couple the photons in the cavity with the qubit, which allows to control or measure the qubit state. The aim of this semester thesis is to design and characterize new microwave Printed Circuit Boards for such cQED experiments. This is motivated by putting more qubits on a device and to let them interact, where every single qubit can be controlled through an external resonator. To do this we need a larger area to put in the superconducting devices on the PCB. Until now, all experiments in the group of Professor Wallraff have been conducted by using 2 x 7 mm chips, with one resonator and 1-2 qubits. To move to experiments involving multiple resonators and qubits, there is a requirement for PCB's with more space, since every single qubit needs a magnetic flux through the loop of the Cooper pair box to tune the transition frequency.

The next chapter of my semester thesis will present the theory behind the coplanar waveguide and the resonator. Chapter 3 will show the new designed PCB's which were constructed with a computer-aided design software (CAD). In the last chapter there will be the results of my measurements of the new PCB's to check them.

2 Theory

A conventional coplanar waveguide which is used on our PCB's can be described by using standard transmission line theory. To build testing devices we have to design some resonators, which can be achieved by putting two gaps, in certain distance, in the waveguide. But also a through transmission line have to be built in order to calibrate the network analyzer in later experiments. The goal of this chapter is to understand the theory of a transmission line and also to develop some important relations in order to analyse the measured data in chapter 4.

2.1 The lumped-element circuit model for a transmission line

To develop a differential equation for the voltage and the current through a two-wire line we want to look at a infinitesimal short piece of line, which can be modeled as a lumped-element circuit:

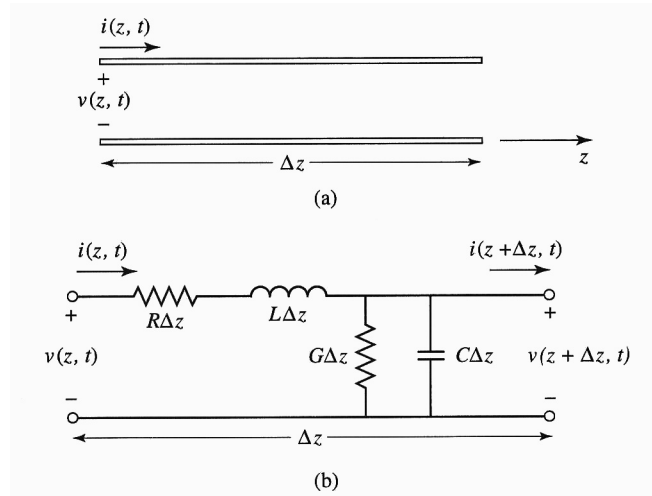


Figure 2.1: Voltage and current definitions and equivalent circuit for an incremental length of transmission line. (a) Voltage and current definitions. (b) Lumped-element equivalent circuit.

where

- R = series resistance per unit length, for both conductors, in Ω/m
- L = series inductance per unit length, for both conductors, in H/m
- G = shunt conductance per unit length, in S/m
- C = shunt capacitance per unit length due to the close proximity of the two conductors, in F/m

notice that $R \neq 0$ even for our low temperature (4.2 K) experiment, since cooper does not become superconducting. G describes the dielectric loss in the material between the conductors.

The calculation can be seen in the appendix. The characteristic impedance Z_0 is defined by

$$Z_0 = \frac{V_0^+}{I_0^+} = \frac{-V_0^-}{I_0^-} \quad (2.1)$$

We find the general solution

$$v(z, t) = V_0^+ e^{-\gamma z + i\omega t} + V_0^- e^{\gamma z + i\omega t} \quad (2.2)$$

$$i(z, t) = \frac{V_0^+}{Z_0} e^{-\gamma z + i\omega t} - \frac{V_0^-}{Z_0} e^{\gamma z + i\omega t} \quad (2.3)$$

$$Z_0 = \frac{R + i\omega L}{\gamma} = \sqrt{\frac{R + i\omega L}{G + i\omega C}} \quad (2.4)$$

It has the same form as a plane wave in a lossy medium, where α describes the rate of decay. With this similarity we can define a wavelength λ and a phase velocity v_p

$$\lambda = \frac{2\pi}{\beta} \quad (2.5)$$

$$v_p = \frac{\omega}{\beta} = \lambda f \quad (2.6)$$

The lossless line fulfills the condition $R=G=0$, see appendix.

2.2 Conventional coplanar waveguide

A coplanar waveguide (CPW) consists of a dielectric substrate with conductors on the top surface. The conductors formed a center strip separated by a narrow gap from two ground planes on either side. If we know the dimensions of the center strip, the gap, the thickness and permittivity of the dielectric substrate we can calculate the effective dielectric constant ϵ_{eff} , characteristic impedance Z_0 and the attenuation α of the line.

2.2.1 Conductor-backed coplanar waveguide

This is just a coplanar waveguide with a lower ground plate as shown in figure (2.2). The lower ground plane provides mechanical strength for a thin and fragile wafer and acts as a heat sink for circuits with active devices. Such a waveguide is called "conductor-backed coplanar waveguide", short CBCPW. The characteristic impedance is determined by the ratio of a/b , the substrate height h and the dielectric constant of the substrate ϵ_r

$$Z_0^{CPW} = \frac{60\pi}{\sqrt{\epsilon_{eff}}} \cdot \frac{1}{\frac{K(k)}{K(k')} + \frac{K(k_3)}{K(k'_3)}} \quad (2.7)$$

where the effective dielectric constant is given by

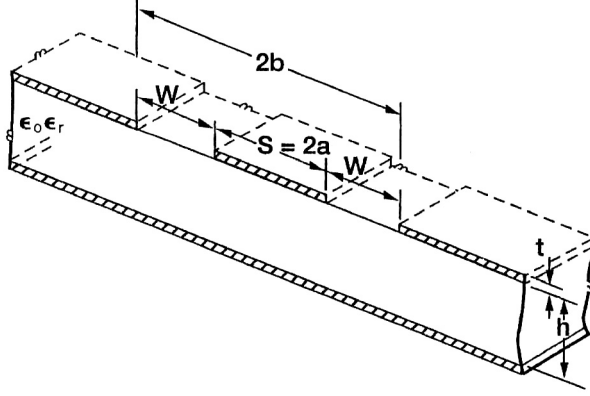


Figure 2.2: Schematic of conductor backed coplanar waveguide (CBCPW).

$$\epsilon_{eff} = \frac{1 + \epsilon_r \tilde{K}}{1 + \tilde{K}} \quad (2.8)$$

$$\tilde{K} = \frac{K(k')K(k_3)}{K(k)K(k'_3)} \quad (2.9)$$

$$k = a/b \quad (2.10)$$

$$k_3 = \frac{\tanh(\frac{\pi a}{2h})}{\tanh(\frac{\pi b}{2h})} \quad (2.11)$$

$$k' = \sqrt{1 - k^2} \quad (2.12)$$

$$k'_3 = \sqrt{1 - k_3^2} \quad (2.13)$$

where K is the complete elliptic integral of the first kind, i.e.

$$K(m) := \int_0^{\pi/2} (1 - m \cdot \sin^2 \Theta)^{-1/2} d\Theta \quad (2.14)$$

Figure below presents the computed ϵ_{eff} and Z_0 as a function of a/b . Notice that in our case $h \ll a, b$ and we can therefore do the approximation $k_3 \approx a/b = k$ and also $k' \approx k'_3$ which lead $\epsilon_{eff} \approx \frac{1+\epsilon_r}{2}$.

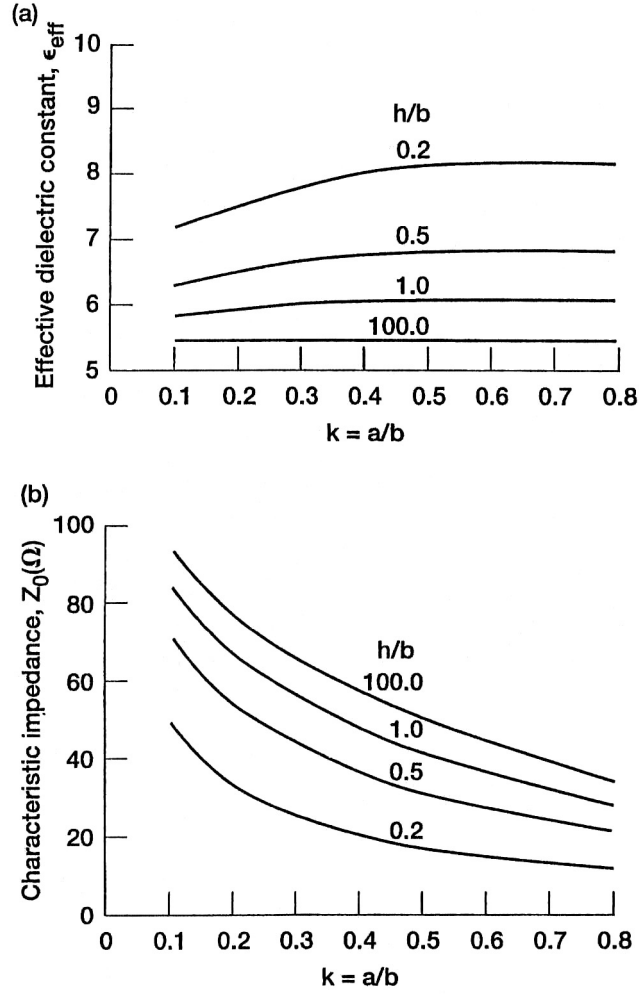


Figure 2.3: Schematic of conductor backed coplanar waveguide (CBCPW).

2.3 parallel RLC resonant circuit

If we cut the CPW such that two equal gaps arise, we have a resonator which is capacitive coupled to the input and output waveguides. Near its resonance frequency it can be modeled by a parallel RLC resonant circuit. We will also therefore discuss first a such a parallel RLC resonator. Figure (2.4) a) shows a RLC resonator

The input impedance is

$$Z_{in} = \left(\frac{1}{R} + \frac{1}{i\omega L} + i\omega C \right)^{-1} \quad (2.15)$$

which is dependent on ω as shown in figure (2.4) b).

As shown in the appendix we can define a resonant frequency by

$$\omega_0 = \frac{1}{\sqrt{LC}} \quad (2.16)$$

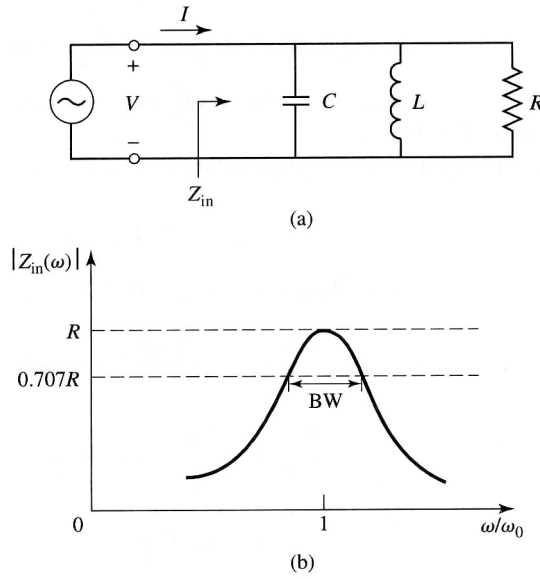


Figure 2.4: A parallel RLC resonator and its response. (a) The parallel RLC circuit. (b) The input impedance magnitude versus frequency.

Another important parameter of a resonant circuit is its quality factor Q , which is defined as

$$Q(\omega) = \omega \cdot \frac{\text{(average energy stored)}}{\text{(energy loss per second)}} \quad (2.17)$$

Thus, $Q(\omega)$ is a measure of the loss of a resonant circuit, i.e. lower loss implies a higher quality factor.

At $\omega = \omega_0$

$$Q(\omega_0) = \omega_0 RC \quad (2.18)$$

This result shows that the Q of a parallel resonant circuit increases as R increases. Near the resonance frequency, the input impedance can be simplified by using $\omega = \omega_0 + \Delta\omega$ where $\Delta\omega$ is small compared to ω_0

$$Z_{in} \approx \frac{R}{1 + 2i\Delta\omega RC} = \frac{R}{1 + 2iQ\Delta\omega/\omega_0} \quad (2.19)$$

When $R \rightarrow \infty$ we can write near the resonance

$$Z_{in} = \frac{1}{2iC(\omega - \omega_0)} \quad (2.20)$$

The effect of loss can be accounted by replacing ω_0

$$\omega_0 \rightarrow \omega_0 \cdot \left(1 + \frac{i}{2Q}\right) \quad (2.21)$$

A resonator with loss can therefore be modeled as a lossless resonator whose resonant frequency ω_0 has been replaced by a complex effective resonant frequency. The half-power bandwidth occurs when the real part of P_{in} is half of the maximum

$$|Z_{in}|^2 = \frac{R^2}{2} \quad (2.22)$$

which, from (2.19), implies

$$\text{bandwidth (BW)} = \frac{1}{Q} \quad (2.23)$$

see figure (2.4) b).

2.4 Loaded and unloaded Q

The quality factor Q is a characteristic of the resonant circuit itself in the absence of any loading effects caused by external circuits and so it is called the unloaded Q. But often, a resonant circuit is coupled to an other external circuit. Figure (2.5) shows a resonator coupled to an external load resistor R_L . If the resonator is a parallel RLC

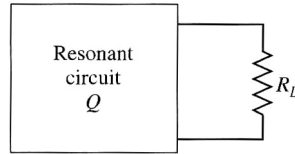


Figure 2.5: A resonant circuit connected to an external load, R_L

circuit, the load resistor R_L combines with R so that the effective resistance is $\frac{RR_L}{R+R_L}$. We can define an external quality factor Q_e as

$$Q_e = \frac{R_L}{\omega_0 L} \quad (2.24)$$

then the loaded Q can be expressed as

$$\frac{1}{Q_L} = \frac{1}{Q_e} + \frac{1}{Q} \quad (2.25)$$

In the measurement the loaded Q_L of the resonator is determined. The unloaded quality factor Q is given by

$$Q = \frac{Q_L}{1 - 10^{-L_0/20}} \quad (2.26)$$

where L_0 is the insertion loss.

2.5 Open-Circuited $\lambda/2$ Line

As mentioned in chapter (2.3) the gaps in a CPW cause a capacitive coupling and therefore build a microwave resonator. Near its resonance frequency ω_0 , such a resonator will behave as a parallel RLC resonator, when the length of the open-circuited

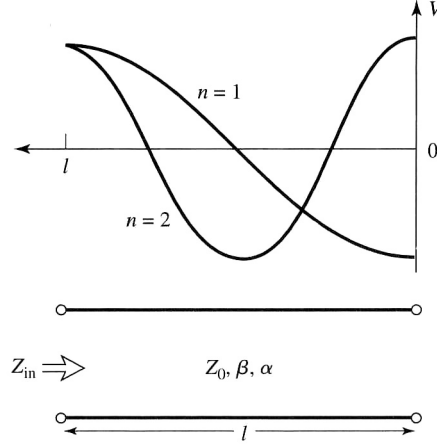


Figure 2.6: An open-circuited length of lossy line, and the voltage distributions for $n = 1$ ($\lambda/2$) and $n = 2$ ($l = \lambda$) resonators

transmission line is $\lambda/2$, or multiples of $\lambda/2$. Consider a lossy transmission line of given length l , which has a characteristic impedance Z_0 , propagation constant β , and an attenuation constant α . The relation between the RLC circuit and the open-circuited $\lambda/2$ line can be expressed as

$$R = \frac{Z_0}{\alpha l} \quad (2.27)$$

$$C = \frac{\pi}{2\omega_0 Z_0} \quad (2.28)$$

$$L = \frac{1}{\omega_0^2 C} \quad (2.29)$$

$$Q = \omega_0 R C = \frac{\pi}{2\alpha l} = \frac{\beta}{2\alpha} \quad (2.30)$$

since $l = \frac{\pi}{\beta}$ at resonance. Where the left-hand side of the equations are the parameters of the RLC circuit.

2.6 Capacitive coupling

The open-circuited $\lambda/2$ line is just connected to the other transmission line by a gap which can be described as a capacitive coupling. We have first to calculate the external quality factor Q_e due to the series $R_L C_g$ -circuit which couples to the resonator. At the resonant frequency

$$Q_e \equiv Q_e(\omega_0) = \frac{\pi}{4Z_0} \cdot \frac{1 + R_L^2 \omega_0^2 C_g^2}{R_L \omega_0^2 C_g^2} \quad (2.31)$$

Now the loaded quality factor of the resonator, Q_L , is found

$$\frac{1}{Q_L} = \frac{1}{Q_e} + \frac{1}{Q} \quad (2.32)$$

where $Q = R\pi/(4Z_0)$

It is useful to define a coefficient of coupling, g , as

$$g = \frac{Q}{Q_e} \quad (2.33)$$

Then, three cases can be distinguished

1. $g < 1$ The resonator is said to be undercoupled to the feedline
2. $g = 1$ The resonator is critically coupled to the feedline
3. $g > 1$ The resonator is said to be overcoupled to the feedline

To obtain maximum power transfer between a resonator and a feedline, the resonator must be matched to the feed at the resonant frequency, this occurs when

$$C_{g,crit} = \frac{1}{\omega_0} \cdot \frac{1}{\sqrt{2Z_0RR_L - R_L^2}} \quad (2.34)$$

3 Designs

The PCB's have been designed with *AutoCAD 2008*. Therefore, the first thing I had to learn was this program. The task was now to design PCB's such that one can put in larger devices, on which the superconducting circuit itself is placed (see figure below).

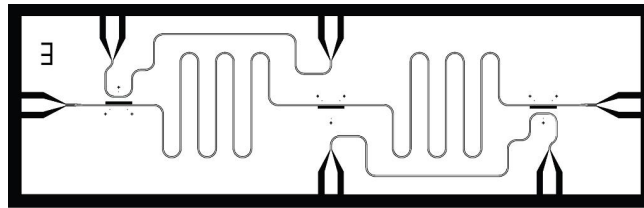
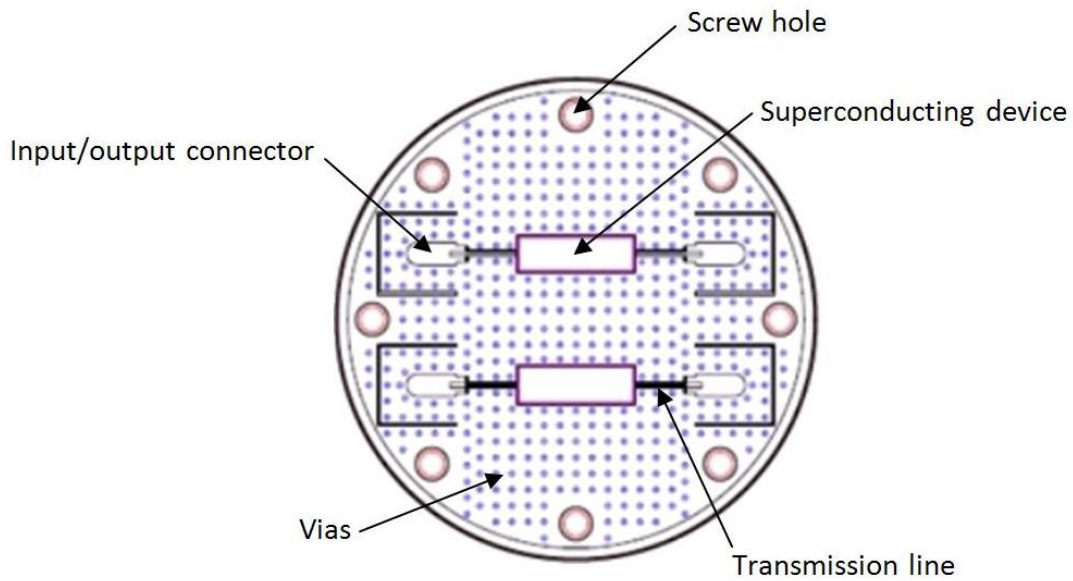
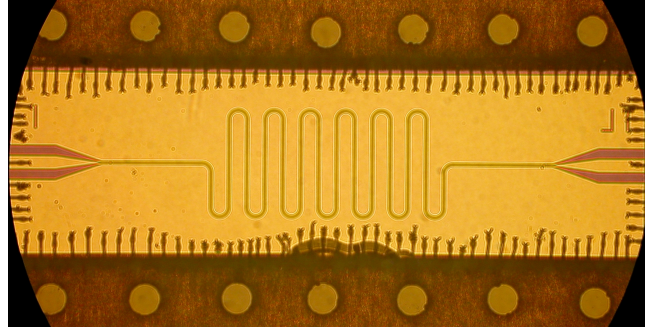


Figure 3.1: A typically superconducting device which is positioned in the middle of the PCB.



Each PCB has 8 holes to fix it with screws to the sample holder. There are 8 fix input/output connectors where the network analyzer is connected to. They all have to be at the same fixed position for every new design. To couple the wave into the waveguide we use a SMP connector which is made of gold with an impedance of 50 Ohm. On each PCB are small holes which are called vias, they are necessary to avoid unwanted resonances due to the coupling to the surface of the board. The frequency range of the network analyzer is 100 MHz to 20 GHz. This equivalent to a wavelength-range of 3 m to 1.5 cm. The distance between the vias has therefore to

be much smaller than 1.5 cm such that no standing wave between them would occur. This unwanted resonances due to the coupling of the incident wave to unwanted parts of the PCB are a big problem also for the qubit-resonators itself, which are placed in the slots. In chapter "Later experiments" one can see in figure (5.2) that due to the additional bonds over the resonator lines a lot of disturbances vanishes up to 10 GHz. In the figure below you see the bonded superconducting device.



3.1 Materials

The microwave printed circuit boards are made of the company *Arlon-Microwave Materials* The used material *AD1000* has the following features:

- Dielectric constant of 10 ± 0.35 at 10 GHz
- high thermal conductivity (0.81 W/mK at 373.15 K)
- electrodeposited cooper on both sides
- low moisture absorption
- dielectric breakdown if voltage exceed 45 kV

The material of the dielectric is woven glass reinforced PTFE/ceramic, PTFE is also known as *Teflon* with a thickness of (0.020 ± 0.002) inches = $(0.020 \pm 0.002) \cdot 25.4$ mm

3.2 Bends

As the length of the resonator is bigger then the size of the PCB we have to wiggle the line. There are many different bends to manage this as shown in figure below. A right-angle bend causes a change in width and therefore a change of the impedance. To compensate such effects of a discontinuity one have to miter the conductor at the bend. In our case, we used a smooth, circular bend with a radius of curvature that is at least several times the width of the line (a minimum value of 3x is often used as a rule of thumb). A disadvantage of such a circular bend (also called "swept bend") is the big amount of space it needs.

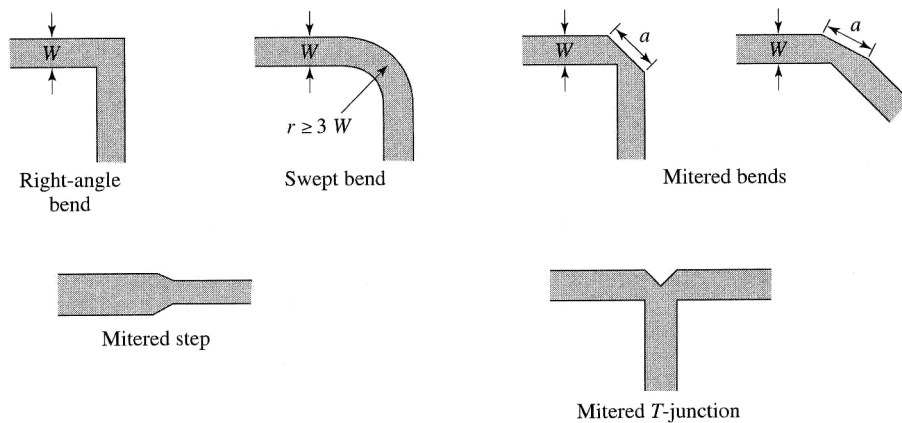


Figure 3.2: Different bend discontinuities and their compensations.

3.3 Different sizes and connectivity of the PCB's

The new PCB's are designed such that the old devices still fit. The connectors are therefore still at the same place, showed in the picture below

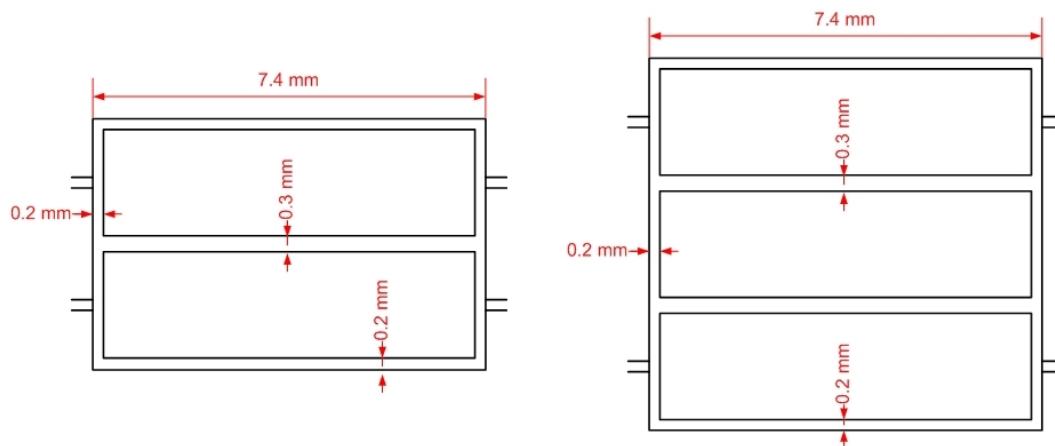
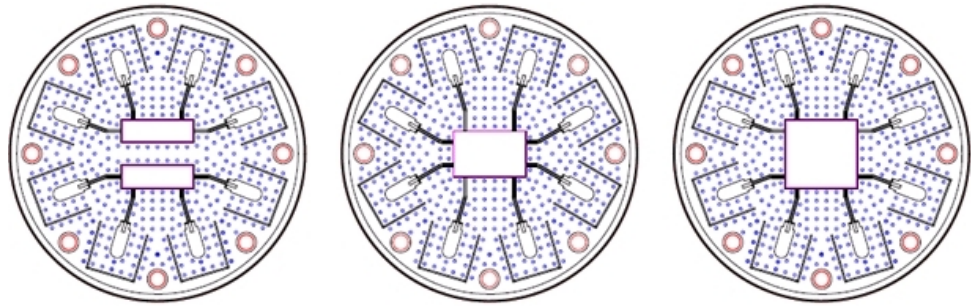
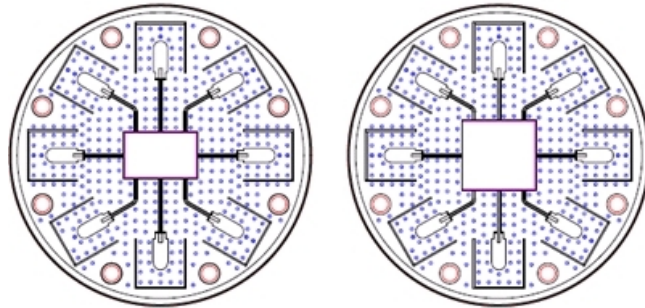


Figure 3.3: left: The slot for 2 old devices and its dimensioning. right: for 3 devices.

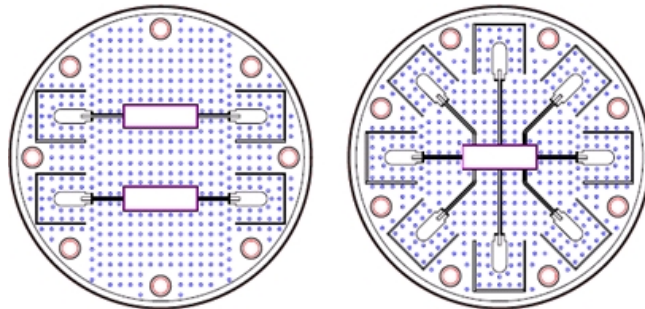
Below are all the different designs. The entry "Design" just describes the arrangement of the connection points, where we start at the top and then goes in the clockwise direction, notice that every side is separate by a colon, e.g. "2:2:2:2" describes a PCB which has 2 connectors on each side. The dimension of the rectangle, which provides the place for the devices, is specified by the entry "Size".



Design	2:1:0:1 and 0:1:2:1	2:2:2:2	2:2:2:2
Size	(7.4 x 2.4) mm	(7.4 x 4.7) mm	(7.4 x 7.0) mm
Devices	2x1	2	3



Design	3:1:3:1	3:1:3:1
Size	(7.4 x 4.7) mm	(7.4 x 7.0) mm
Devices	2	3



Design	0:1:0:1 and 0:1:0:1	3:1:3:1
Size	2x(7.4 x 2.4) mm	(7.4 x 7.0) mm
Devices	2x1	1

There are also 2 designs where the cut-outs are apart, such that some vias are now between them. This is motivated by the smaller coupling between the two devices. The next 7 designs are testing boards where we have two different kinds of building a capacitor: overlapping of the transition lines and a gap in the transition line. By using the old designs we know that a resonator-length of 12.71 mm correspond a 6 GHz resonance frequency. Since there is a linear relation between the wavelength and the frequency of an electromagnetic wave we can easily calculate the resonator-length for other resonances. Since the real physical dimension of the length L_0 is larger than

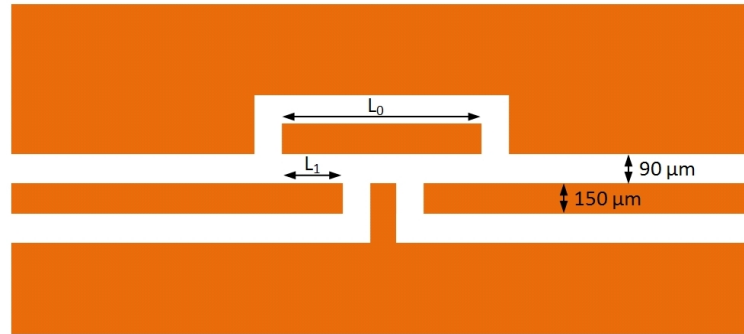


Figure 3.4: Overlap-design. The orange area is made of copper.

the board itself, we have to wiggle it. But to avoid disturbing reflections in the curve of a wiggle, the radius of the swept bend is larger than 3 times the width of the line (as discussed in the chapter about "Bends").

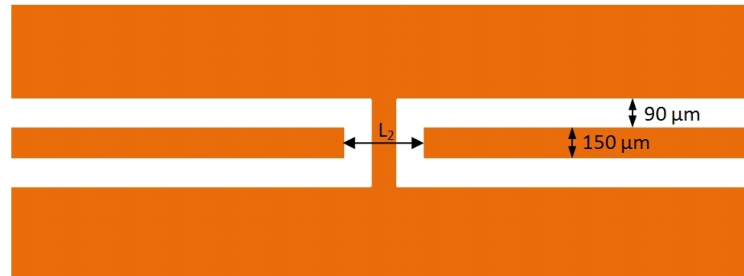


Figure 3.5: Gap-design. The orange area is made of copper.

	L_0	L_1	L_2
4.5 GHz	16.95 mm	410 μm	90 μm
5.25 GHz	15.25 mm	410 μm	90 μm
6 GHz	12.71 mm	410 μm	90 μm

This designs can now be simulated by a program called "Maxwell 3D" to calculate the capacitances. One has to draw the capacitor with its dimension and the computer then calculate the capacitances numerically

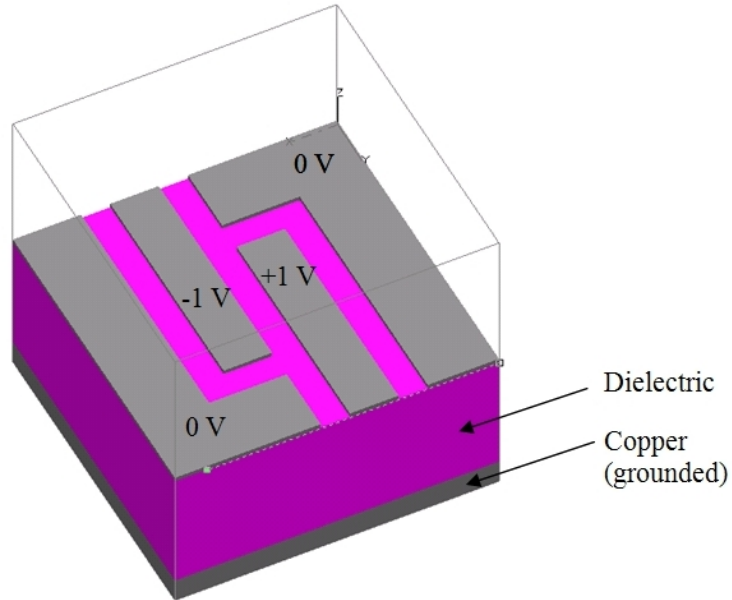
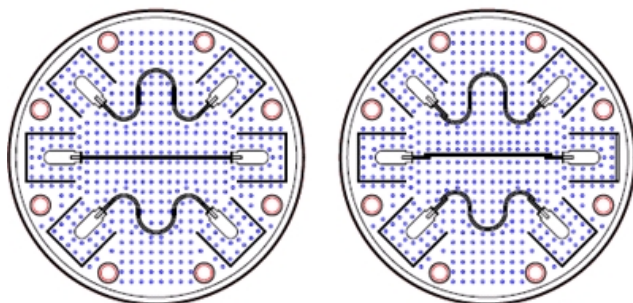


Figure 3.6: Draw of the overlap capacitor in "Maxwell 3D"

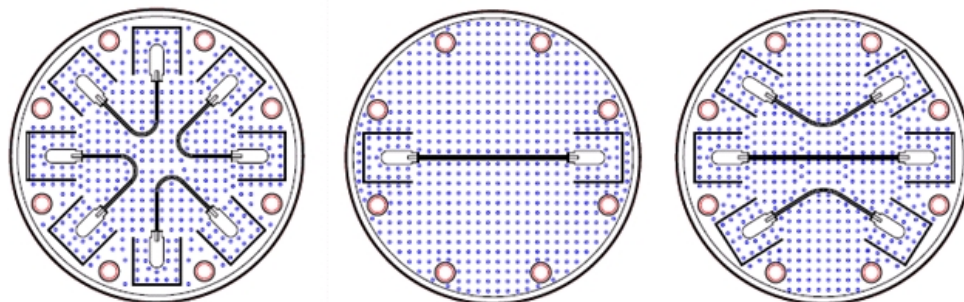
	C_g
gap	$(6.667 \pm 1.7\%) fF$
overlap	$(23.13 \pm 1.3\%) fF$

By the way: The dimensions of the transmission lines are such that the impedance of the waveguide is about 50 Ohm. For $h = 500 \mu m$, $2a = 150 \mu m$, $w = 90 \mu m$ and $\epsilon_r = 10$ (see figure (2.2)) we can use equation (2.7) to get $Z_0^{CPW} = 54.4 \Omega$.

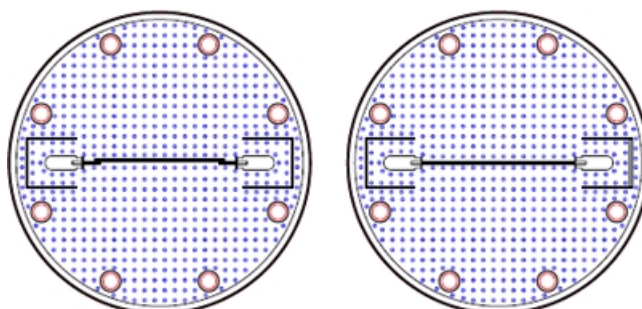
To calibrate the network analyzer we have to measure the dispersion relation of the through lines, this can be done by the 3 different designs of the direct connected lines.



Capacitor design	gap	overlap
Resonance frequencies	(4.5 / 6.0 / 5.25) GHz	(4.5 / 6.0 / 5.25) GHz



Through lines	4	1	3
---------------	---	---	---



Capacitor design	overlap	gap
Resonance frequency	6.0 GHz	6.0 GHz

4 Measurements and characterization

The designs describe in the previous chapter were manufactured by *Hughes Circuits Inc.* All the experiments were accomplished in liquid helium with a temperature of $T=4.2$ K. The devices which will have put in later experiments are made of a niobium thin film. Niobium has the advantage that it has a critical temperature where it gets superconducting of $T_c=9.2$ K which is above the temperature of liquid helium. A second advantage is that some effects due to the temperature would be suppressed. The network analyzer was calibrated with the coaxial lines from its ports to the dipstick. In this chapter, measurements of the test PCB's are described and characterized.

4.1 Calibration

Firstly, a calibration for the network analyzer with the 1-8-cables was measured

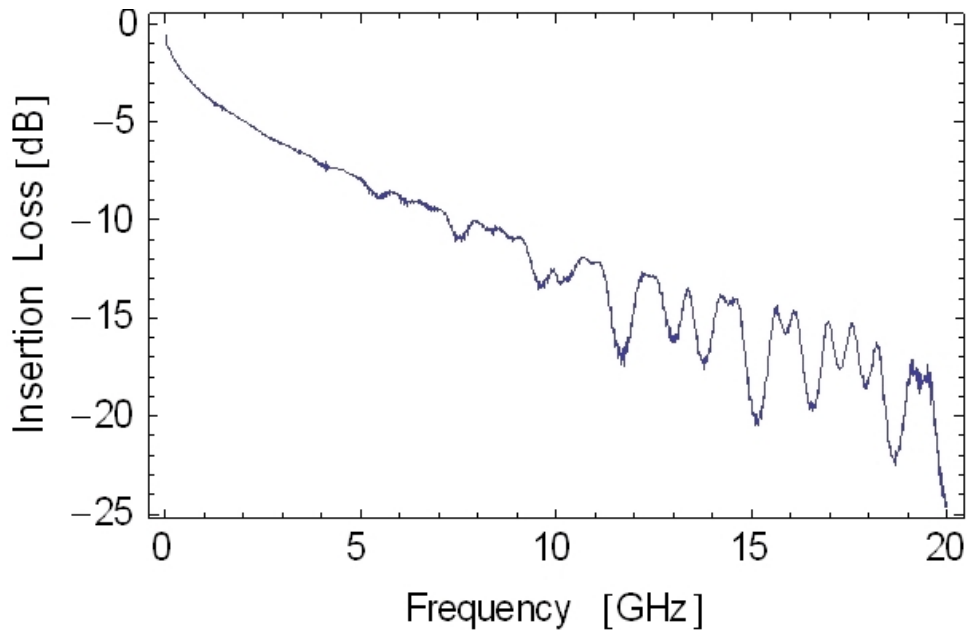


Figure 4.1: Calibration for the network analyzer with the 1-8-cables

Insertion loss is the decrease in transmitted signal power. This is a typically calibration line of a wave guide. If we connect two ports without a transmission line between we can observe the following plot

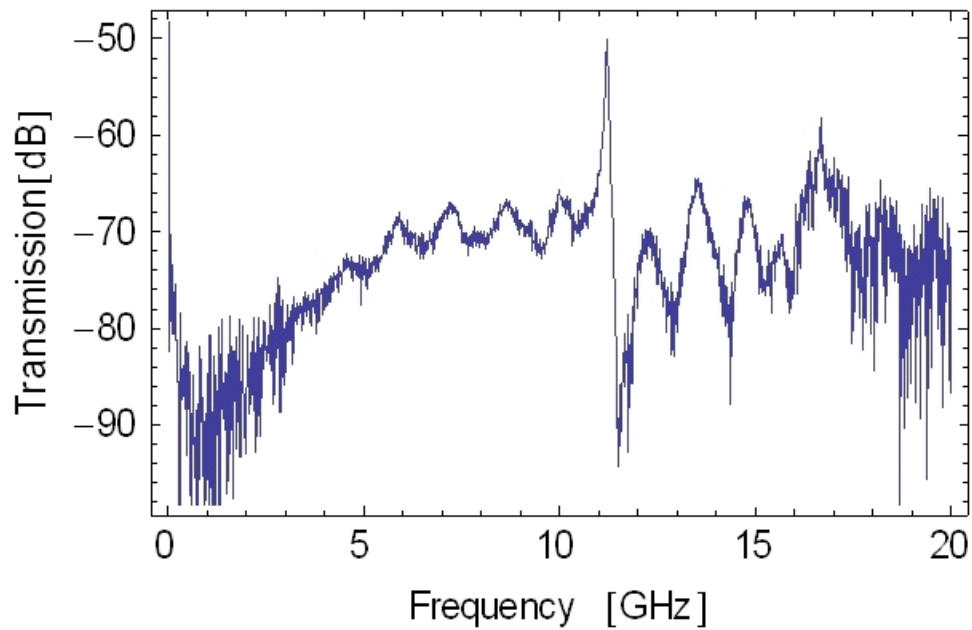


Figure 4.2: No connection between the two ports

The insertion loss is very high compared to the connected cables. There is a strong peak around 11 GHz which is due to the resonance frequency of the sample holder, this can be modeled by a Lorentzian fit

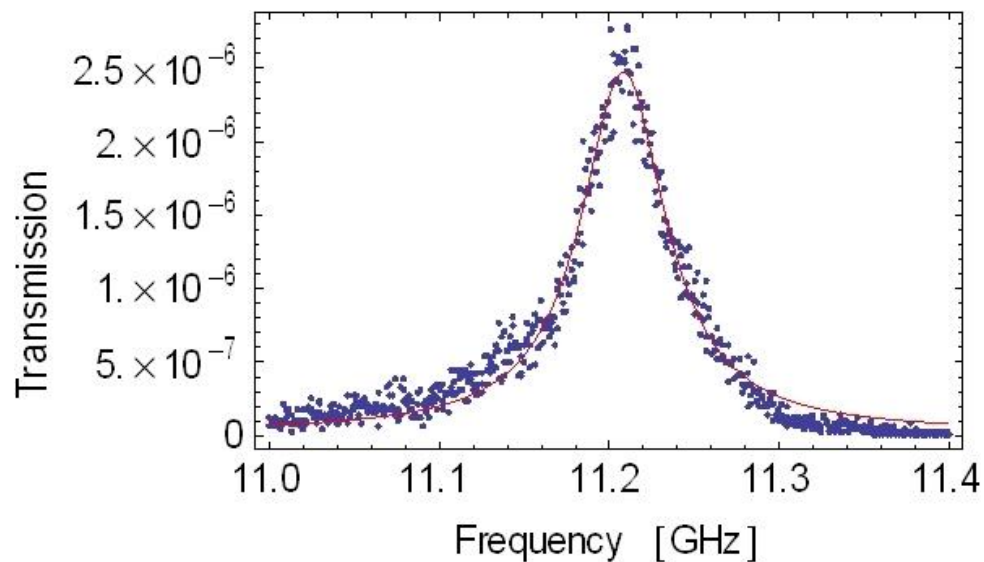


Figure 4.3: Lorentzian fit of the sample holder resonance

Notice that the transmission-plot without any units is the relative transmission, i.e. 0 means that no signal goes through and 1 correspond to a full transition. The Lorentzian fit has calculated with Mathematica with the following results

Frequency [GHz]	11.208
Quality factor	184
Peak insertion loss [dB]	-56.1

4.2 Resonator measurements

The next measurements are the resonator. We only consider the 5.25 GHz resonance of the overlapping capacitor design with its plots, because all the other analysis are of the same kind and therefore only tabulated at the end. Firstly the whole range (100 MHz to 20 GHz) of the transmission

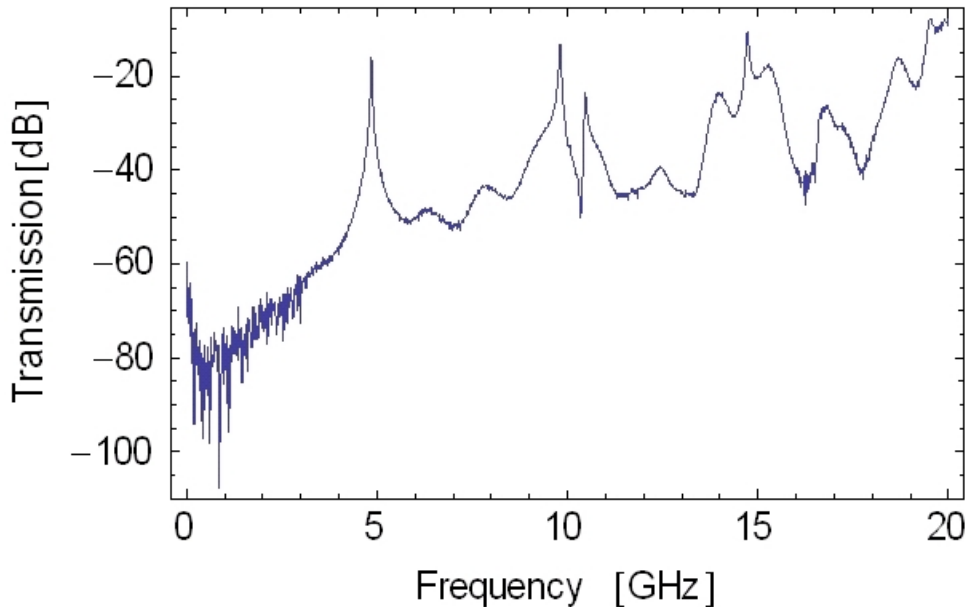


Figure 4.4: Testing board with 3 capacitors (overlapping design) on it, here 1-7-cables with a theoretically resonance frequency at 5.25 GHz

The first peak is the wanted resonance, the second one is the first harmonic with doubled resonance frequency (around 9.7 GHz) and the third peak describes the sampled holder resonance. But now we are interested in the fundamental resonance caused by the capacitor which can be fit by a Lorentzian curve

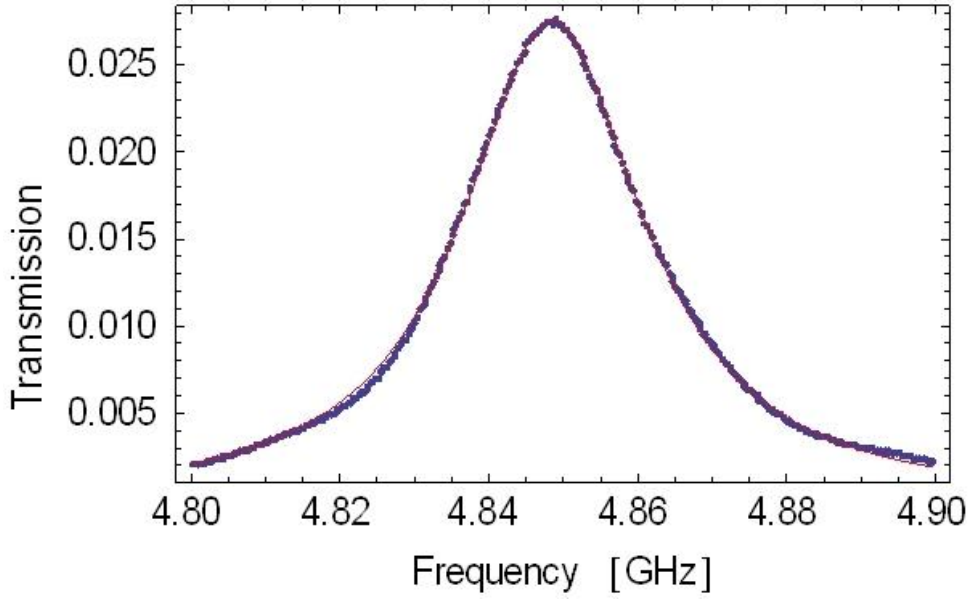


Figure 4.5: Lorentzian fit of the 5.25 GHz resonance

The experimental resonance frequency is lowered by around 400 MHz. Since the capacitors has been calculated and constructed at room temperature we have also performed the experiment at room temperature

5.25 GHz	liquid Helium	Room temperature
Frequency [GHz]	4.849	5.098
Peak insertion loss [dB]	-15.6	-29.5
Q_L	165	62
Q	198	64
Q_e	990	1984
$g = Q/Q_e$	0.20	0.03
Measured C_g [fF]	18.50	12.43
ϵ_r	7.92	7.07

At room temperature the resonance frequency increases compared to the fluid helium, but the quality factor and the maximum insertion loss decrease. The resonance frequency is still smaller than the theoretical expected value of 5.25 GHz.

The measured quality factors Q_L are lower than the expected external quality factors. This is probably due to the non vanishing internal quality factor. But we can use the equation (2.26) to calculate the internal quality factor and with equation (2.31) the gap capacitance can then be calculated, as you can see in the table above. It stands out the big difference of the external quality factors in the two temperatures, this means that due to the increased thermal fluctuations the peak is smeared out.

The dielectric constant of the material can also be read out of the data:

$c = f \cdot \lambda \cdot \sqrt{\epsilon_{eff}}$, where f is the frequency, c is the speed of light in the vacuum and the resonator length is half of the wavelength. Now, the dielectric constant of the substrate can be determined by equation (2.8) which is lower than the predicted one.

The 4.5 GHz and 6.0 GHz resonances have the following properties

4.5 GHz	liquid Helium	Room temperature
Frequency [GHz]	4.208	4.431
Peak insertion loss [dB]	-18.9	-32.8
Q_L	220	65
Q	248	67
Q_e	1949	2178
$g = Q/Q_e$	0.13	0.03
Measured C_g [fF]	15.19	13.64
ϵ_r	7.71	6.86

6.0 GHz	liquid Helium	Room temperature
Frequency [GHz]	5.410	5.707
Peak insertion loss [dB]	-15.5	-28.9
Q_L	157	63
Q	189	65
Q_e	927	2048
$g = Q/Q_e$	0.20	0.03
Measured C_g [fF]	17.13	11.40
ϵ_r	8.36	7.42

It is very important, that the 3 resonators on the PCB doesn't influence each other. To check that, one can plot all the resonator-transmissions in one diagram and as you can see in the plot below, there are no additional resonances on each frequency. This means that the resonators are insulated from the others.

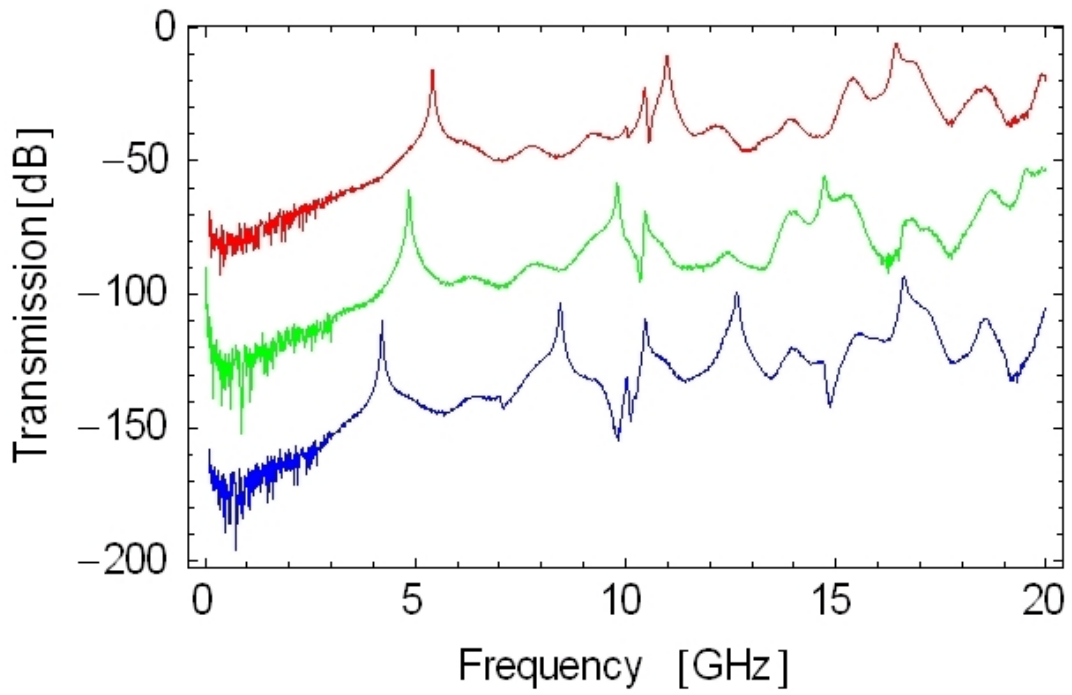


Figure 4.6: The 3 resonators in one plot (red: 6 GHz, green: 5.25 GHz and offset=-45 dB, blue: 4.5 GHz and offset=-90 dB)

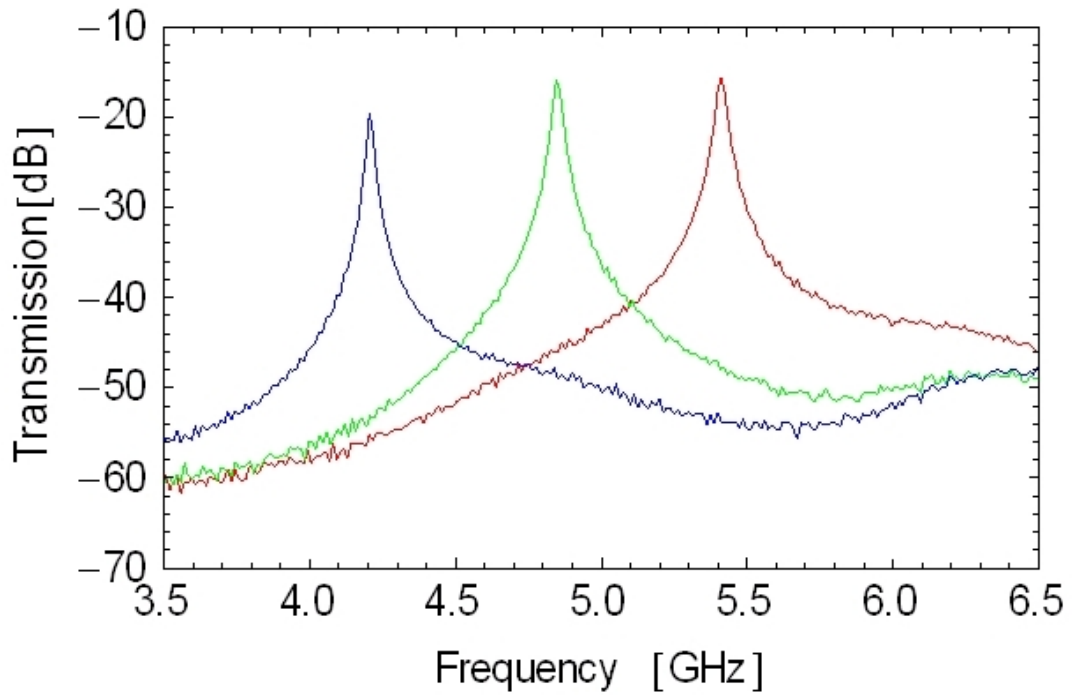


Figure 4.7: The resonance of the 3 different resonator-designs (red: 6 GHz, green: 5.25 GHz, blue: 4.5 GHz)

In section (2.6) we distinguished the strength of the coupling, i.e. to obtain maximum power transfer between a resonator and a feedline, the coefficient of coupling should be 1. This can be reached if $Q \gg Q_e$. This also means that the loaded quality factor (this is what we measured) should be given by the external one. The theoretical external quality factor can be calculated by (2.31), where C_g was determined by a simulation program called "Maxwell 3D"

	4.5 GHz	5.25 GHz	6.0 GHz
calculated Q_e	737	542	415
measured Q_e	1949	990	927

where $C_g = (23.128 \pm 1.3\%) fF$, and this is much smaller than the gap capacitance which was calculated based on the measured data. But there is a small fluctuation of the C_g for the different frequency at the same temperature (!). You can also see the big difference of the calculated gap capacitance for the two different temperatures due to the extension of the material. The measured quality factors are bigger than the expected external quality factors. This is probably due to the non vanishing internal quality factor.

5 Later experiments

Lars Steffen did a resonator measurement on the PCB with double sized cut-out on July 2008. To test whether one can use this PCB to measure two resonators which lie next to each other (without any additional ground plane of the PCB between the resonators chips), two resonators with fundamental frequencies of 3.25 GHz and 6.4 GHz respectively were mounted onto the PCB and measured in liquid helium at 4.2 K. The figure below shows schematically the new PCB with the port numbers and the resonators.

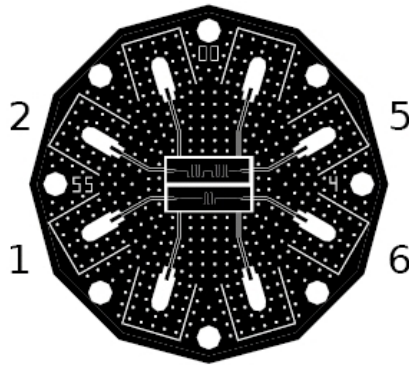


Figure 5.1: Schematic of the PCB with the resonators. Numbers on the side indicate port numbers.

The next figure shows the measurement of the two resonators and the crosscoupling. The graph on the top shows the measurement of the configuration where the resonators are just bonded on the sides of the chip, either to the PCB or to the other chip. The graph on the bottom shows the same devices but with additional bonds over the resonator lines. The blue lines show the measurement of the resonator with the fundamental frequency 6.4 GHz (ports 1-6), the red lines belong to the resonator with fundamental frequency 3.25 GHz (ports 2-5) and the green lines show the cross coupling between ports 1-2 (dark) and ports 1-5 (bright). The grid lines indicate the fundamental and harmonic frequencies of the 3.25 GHz resonator. From measurements above the critical temperature of niobium (9.2 K) one can identify the resonance at 9.45 GHz (dashed line) as a resonance from the sample holder.

In the device without additional bonds over the resonator, there are extra resonances at 4.2 GHz, 7.3 GHz, 7.9 GHz, 11.4 GHz, 11.85 GHz and some above 12 GHz. By applying additional bonds over the resonator, all but one (at 11.77 GHz) extra resonance below 12 GHz disappear.

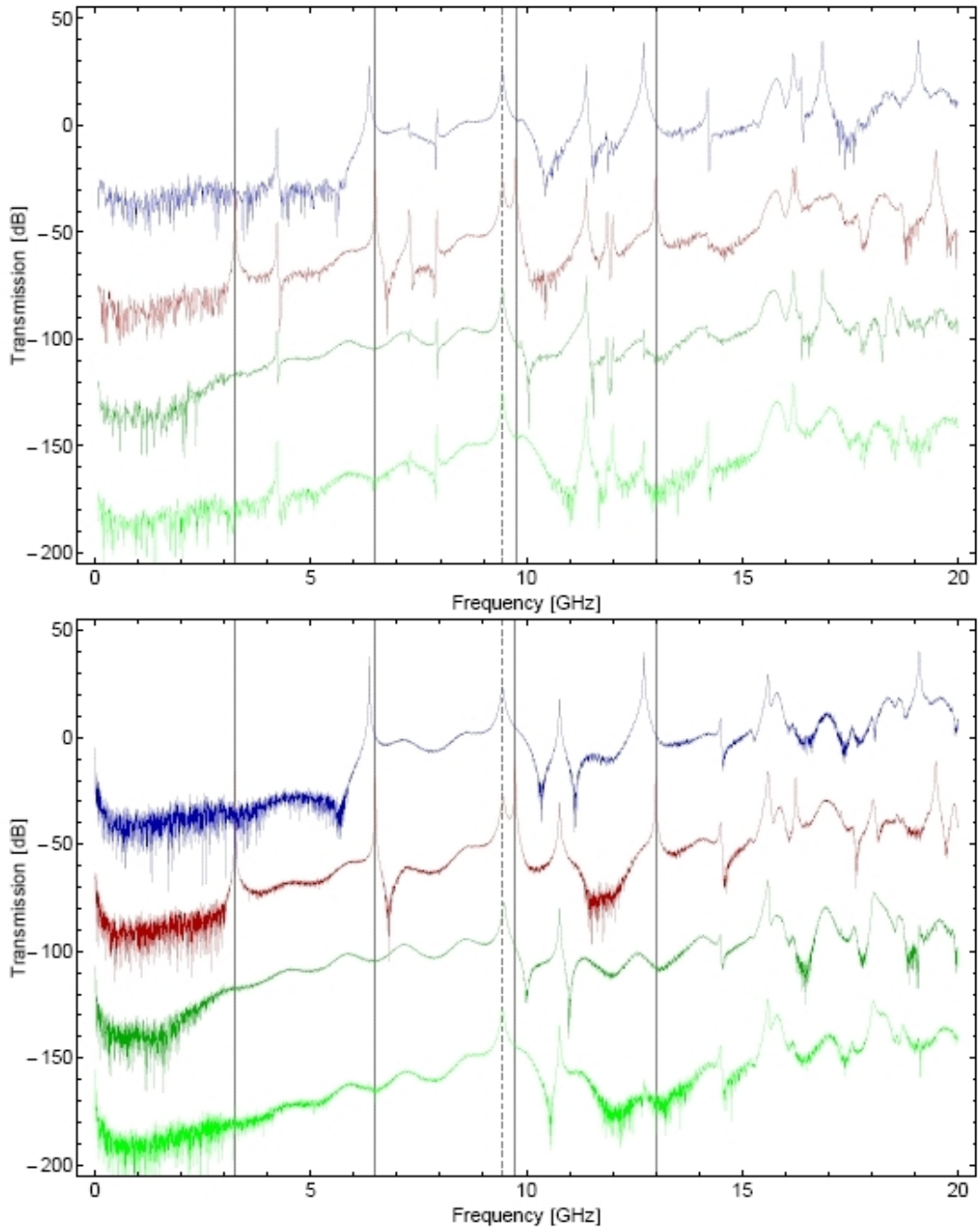


Figure 5.2: Measurements of the resonators (blue: 6.4 GHz, red: 3.25 GHz) and cross couplings (dark green: ports 1-2, light green: ports 1-5) without (top) and with (bottom) additional bonds over the resonator lines. The measurements have different offsets for better distinction. The solid grid lines indicate the fundamental and harmonics of the 3.25 GHz resonator, the dashed line indicates a sampleholder resonance.

6 Conclusion

The main goal of this thesis was to design bigger PCB's for later experiments. There were some designs to calibrate the network analyzer and also resonators with two different designs: overlapping and gap capacitor. Measuring the overlapping capacitors showed that the resonance frequency is always lower than the expected value, also the capacitance is lower than the simulated value, but still in the same order of magnitude. But since the experiments were also done at room temperature, one can see a strong dependence on temperature. The calculated dielectric constant was lower than the one given by the manufacturer, therefore I suppose that the difference is due to the imprecise cutting-out of the machine. Another important fact is the non interacting of the different resonators which are placed on the same PCB, this can be explained by the big density of the vias, which avoid standing waves in the frequency range of the network analyzer.

7 Appendix

7.1 The lumped-element circuit model for a transmission line

By using the two Kirchhoff laws we get

$$v(z, t) - R \cdot \Delta z \cdot i(z, t) - L \cdot \Delta z \frac{\partial i(z, t)}{\partial t} - v(z + \Delta z, t) = 0 \quad (7.1)$$

$$i(z, t) - G \cdot \Delta z \cdot v(z + \Delta z, t) - C \cdot \Delta z \frac{\partial v(z + \Delta z, t)}{\partial t} - i(z + \Delta z, t) = 0 \quad (7.2)$$

taking the limit $\Delta z \rightarrow 0$ yields the following differential equations

$$\frac{\partial v(z, t)}{\partial z} = -R \cdot i(z, t) - L \cdot \frac{\partial i(z, t)}{\partial t} \quad (7.3)$$

$$\frac{\partial i(z, t)}{\partial z} = -G \cdot v(z, t) - C \cdot \frac{\partial v(z, t)}{\partial t} \quad (7.4)$$

which are called *telegrapher equations*.

By assuming that we can separate the solutions in a z - and t depending part, i.e.

$$i(z, t) = I(z)e^{i\omega t} \quad (7.5)$$

$$v(z, t) = V(z)e^{i\omega t} \quad (7.6)$$

the differential equations then simplify to

$$\frac{dV(z)}{dz} = -(R + i\omega L)I(z) \quad (7.7)$$

$$\frac{dI(z)}{dz} = -(G + i\omega C)V(z) \quad (7.8)$$

This equations can be solved by the following Ansatz

$$I(z) = I_0^+(z)e^{-\gamma z} + I_0^-(z)e^{\gamma z} \quad (7.9)$$

$$V(z) = V_0^+(z)e^{-\gamma z} + V_0^-(z)e^{\gamma z} \quad (7.10)$$

$$\gamma = \alpha + i\beta = \sqrt{(R + i\omega L)(G + i\omega C)} \quad (7.11)$$

which represent a superposition of two waves with opposite direction of propagation. Inserting the above Ansatz into the differential equation we find the general solution.

7.2 The Lossless Line

If we neglect any loss of the line, the solution simplifies by setting $R = G = 0$

$$v(z, t) = V_0^+ e^{-i(\beta z - \omega t)} + V_0^- e^{i(\beta z + \omega t)} \quad (7.12)$$

$$i(z, t) = \frac{V_0^+}{Z_0} e^{-i(\beta z - \omega t)} - \frac{V_0^-}{Z_0} e^{i(\beta z + \omega t)} \quad (7.13)$$

$$Z_0 = \sqrt{\frac{L}{C}} \quad (7.14)$$

$$\gamma = \alpha + i\beta = i\omega\sqrt{LC} \quad (7.15)$$

As expected for the lossless case, the attenuation constant α is zero. Also the wavelength and the phase velocity simplify by

$$\lambda = \frac{2\pi}{\beta} = \frac{2\pi}{\omega\sqrt{LC}} \quad (7.16)$$

$$v_p = \frac{\omega}{\beta} = \frac{1}{\sqrt{LC}} \quad (7.17)$$

7.3 parallel RLC resonant circuit

The complex power delivered to the resonator is

$$P_{in} = \frac{1}{2} |V|^2 \left(\frac{1}{R} + \frac{i}{\omega L} - i\omega C \right) \quad (7.18)$$

and the power dissipated by the resistor R is given by

$$P_{loss} = \frac{1}{2} \frac{|V|^2}{R} \quad (7.19)$$

notice that $V \equiv V(\omega)$. And the average magnetic energy stored in the inductor L is

$$W_m = \frac{1}{4} |V|^2 \frac{1}{\omega^2 L} \quad (7.20)$$

Resonance occurs when $W_m(\omega_0) = W_e(\omega_0)$ which is fulfilled if

$$C = \frac{1}{\omega_0^2 L} \Rightarrow Z_{in}(\omega_0) = R \quad (7.21)$$

that implies the resonant frequency ω_0 which should therefore be defined as

$$\omega_0 = \frac{1}{\sqrt{LC}} \quad (7.22)$$

Another important parameter of a resonant circuit is its quality factor Q , which is defined as

$$Q(\omega) = \omega \cdot \frac{(\text{average energy stored})}{(\text{energy loss per second})} \quad (7.23)$$

$$= \omega \cdot \frac{W_m + W_e}{P_{loss}} \quad (7.24)$$

Thus, $Q(\omega)$ is a measure of the loss of a resonant circuit, i.e. lower loss implies a higher quality factor.

At $\omega = \omega_0$ we can use the fact that $W_m = W_e$ to calculate the quality factor

$$Q(\omega_0) \equiv \omega_0 \cdot \frac{2 \cdot W_m}{P_{loss}} = \omega_0 RC \quad (7.25)$$

7.4 Open-Circuited $\lambda/2$ Line

The input impedance of an open-circuited line of length l is

$$Z_{in} = Z_0 \coth(\alpha + i\beta)l = Z_0 \frac{1 + i \tan(\beta l) \tanh(\alpha l)}{\tanh(\alpha l) + i \tan(\beta l)} \quad (7.26)$$

where we used an identity for the hyperbolic tangent. Observe that $Z_{in} = iZ_0 \tan(\beta l)$ if $\alpha = 0$, i.e. no loss. Assume that $l = \lambda/2$ at $\omega = \omega_0$, and let $\omega = \omega_0 + \Delta\omega$ and assume that $\alpha l \ll 1$ and so $\tanh(\alpha l) \approx \alpha l$. Then,

$$\beta l = \frac{\omega l}{v_p} = \frac{\omega_0 l}{v_p} + \frac{\Delta\omega l}{v_p} \quad (7.27)$$

$$\frac{\lambda}{v_p} = \frac{2\pi}{\omega_0} \quad (7.28)$$

$$\beta l = \pi + \frac{\pi \cdot \Delta\omega}{\omega_0} \quad (7.29)$$

$$\Rightarrow \tan(\beta l) = \tan\left(\pi + \frac{\Delta\omega \cdot \pi}{\omega}\right) = \tan\left(\frac{\Delta\omega \cdot \pi}{\omega}\right) \approx \frac{\Delta\omega \cdot \pi}{\omega_0} \quad (7.30)$$

using this result for Z_{in} gives

$$Z_{in} = \frac{Z_0}{\alpha l + i(\Delta\omega\pi/\omega_0)} \quad (7.31)$$

by comparing with the input impedance of the RLC circuit as given by (2.19) suggests the equivalent relation.

7.5 Capacitive coupling

A series $R_L C_g$ -circuit has the following impedance

$$Z_{RC} = R_L - \frac{i}{\omega C_g} \quad (7.32)$$

$$P_{loss} = \frac{1}{2} R_L |I|^2 \quad (7.33)$$

The average energy stored by the resonator with capacitance C

$$\text{average energy stored} = \frac{1}{2} C |V|^2 \quad (7.34)$$

$$(7.35)$$

By using that $R_L = \text{Re}(Z_{RC})$ and $|Z_{RC}|^2 = |V/I|^2$ we can calculate a frequency depending quality factor for the RC-circuit

$$Q_e(\omega) = \omega \cdot \frac{\frac{1}{2}C |V|^2}{\frac{1}{2}\text{Re}(Z_{RC}) |I|^2} = \omega \cdot \frac{C |Z_{RC}|^2}{\text{Re}(Z_{RC})} = \omega \cdot \frac{C}{\text{Re}(1/Z_{RC})} \quad (7.36)$$

notice that $1/Z_{RC}$ is called the *admittance*. This leads to the external quality factor at the resonance frequency

$$Q_e(\omega) = \frac{1 + R_L^2 \omega^2 C_g^2}{R_L \omega C_g^2} \cdot C \quad (7.37)$$

At the resonance frequency ω_0 we can write for the capacitance $C = \pi/(4\omega_0 Z_0)$, where the additional 1/2-factor occurs due the assumption that the resonator is symmetrically coupled to the in- and output line and we only look at one side coupling

$$Q_e \equiv Q_e(\omega_0) = \frac{\pi}{4Z_0} \cdot \frac{1 + R_L^2 \omega_0^2 C_g^2}{R_L \omega_0^2 C_g^2} \quad (7.38)$$

List of Figures

2.1	Voltage and current definitions and equivalent circuit for an incremental length of transmission line. (a) Voltage and current definitions. (b) Lumped-element equivalent circuit.	3
2.2	Schematic of conductor backed coplanar waveguide (CBCPW).	5
2.3	Schematic of conductor backed coplanar waveguide (CBCPW).	6
2.4	A parallel RLC resonator and its response. (a) The parallel RLC circuit. (b) The input impedance magnitude versus frequency.	7
2.5	A resonant circuit connected to an external load, R_L	8
2.6	An open-circuited length of lossy line, and the voltage distributions for $n = 1$ ($\lambda/2$) and $n = 2$ ($l = \lambda$) resonators	9
3.1	Different bend discontinuities and their compensations.	13
3.2	left: The slot for 2 old devices and its dimensioning. right: for 3 devices.	13
3.3	Overlap-design. The orange area is made of copper.	14
3.4	Gap-design. The orange area is made of copper.	15
3.5	Draw of the overlap capacitor in "Maxwell 3D"	16
4.1	Calibration for the network analyzer with the 1-8-cables	18
4.2	No connection between the two ports	19
4.3	Lorentzian fit of the sample holder resonance	19
4.4	Testing board with 3 capacitors (overlapping design) on it, here 1-7-cables with a theoretically resonance frequency at 5.25 GHz	20
4.5	Lorentzian fit of the 5.25 GHz resonance	21
4.6	The 3 resonators in one plot (red: 6 GHz, green: 5.25 GHz and offset=-45 dB, blue: 4.5 GHz and offset=-90 dB)	23
4.7	The resonance of the 3 different resonator-designs (red: 6 GHz, green: 5.25 GHz, blue: 4.5 GHz)	23
5.1	Schematic of the PCB with the resonators. Numbers on the side indicate port numbers.	25
5.2	Measurements of the resonators (blue: 6.4 GHz, red: 3.25 GHz) and cross couplings (dark green: ports 1-2, light green: ports 1-5) without (top) and with (bottom) additional bonds over the resonator lines. The measurements have different offsets for better distinction. The solid grid lines indicate the fundamental and harmonics of the 3.25 GHz resonator, the dashed line indicates a sampleholder resonance.	26

Bibliography

- [1] David M. Pozar, *Microwave engineering*, John Wiley and Sons, third edition, 2005.
- [2] Michael A. Nielsen and Isaac L. Chuang, *Quantum Computation and Quantum Information*, Cambridge University Press, 2000.
- [3] Andreas Wallraff, Hannes Majer, Luigi Frunzio, Rob Schoelkopf *Superconducting solid state cavity quantum electrodynamics*.
- [4] Lars Steffen, *Local Qubit Control in Circuit Quantum Electrodynamics*, diploma thesis, 2008.
- [5] Raoul Scherwitzl, *Characterization of superconducting resonators*, semester thesis, 2007.
- [6] Arthen/Weber, *Mathematical Methods for physicists*, Harcourt academic press, page 355.
- [7] Rainee N. Simons, *Coplanar Waveguide Circuits Components and Systems*, Wiley-IEEE Press, first edition, 2001.